

### Supplementary figure legends:

#### **Fig S1. The impact of paclitaxel resistance on ABCB1, ABCC1 and ABCC3 expression and distribution inside A549 cells**

(A) ABCB1, ABCC1, ABCC3 and ABCC10 were visualized in non-resistant and paclitaxel-resistant A549 cells by immunocytochemical staining followed by confocal microscopy. Green fluorescence of ABC transporters is derived from Alexafluor488-conjugated secondary antibody, blue DNA was stained with DAPI, whereas lysosomes in red were stained with LysoTracker™ Deep Red. (B and C) The fluorescence intensity, which corresponds to ABC protein level inside cells (B) and colocalization between considered proteins and lysosomes (C) were determined in arbitrary units (a.u.) with Leica Application Suite X. The difference between two means was tested with Student's t-test or Mann Whitney test, and statistically significant differences are marked with \* when  $p < 0.05$ , \*\* when  $p < 0.01$ , \*\*\* when  $p < 0.001$ .

(D) Western blot images of SDS-PAGE separated proteins from whole cell lysates were acquired with ChemiDoc-IT2 (UVP, Meranco, Poznan, Poland). ACTB served as a loading control.

#### **Fig S2. The impact of paclitaxel resistance on ABCB1, ABCC1 and ABCC3 expression and distribution inside MDA-MB-231 cells**

(A) ABCB1, ABCC1, ABCC3 and ABCC10 were visualized in non-resistant and paclitaxel-resistant A549 cells by immunocytochemical staining followed by confocal microscopy. Green fluorescence of ABC transporters is derived from Alexafluor488-conjugated secondary antibody, blue DNA was stained with DAPI, whereas lysosomes in red were stained with LysoTracker™ Deep Red. (B and C) The fluorescence intensity, which corresponds to ABC protein level inside cells (B) and colocalization between considered proteins and lysosomes (C) were determined in arbitrary units (a.u.) with Leica Application Suite X. The difference between two means was tested with Student's t-test or Mann Whitney test, and statistically significant differences are marked with \* when  $p < 0.05$ , \*\* when  $p < 0.01$ , \*\*\* when  $p < 0.001$ .

(D) Western blot images of SDS-PAGE separated proteins from whole cell lysates were acquired with ChemiDoc-IT2 (UVP, Meranco, Poznan, Poland). ACTB served as a loading control.

#### **Fig S3. Confocal microscopy imaging of lysosomal proteins**

Confocal microscopy imaging of lysosomal proteins in non- and paclitaxel-resistant cancer cell lines A549 (A) and MDA-MB-231 (B). ABC transporters were visualized by immunocytochemical staining followed by confocal microscopy. Red fluorescence of ABC transporters is derived from Alexa Fluor®546 R-labelled secondary antibody and LAMP1- green fluorescence is derived from Alexafluor488-conjugated secondary antibody. The scans of lysosomes were deconvolved using 3D-Deconvolution accessible in Leica Application Suite X software (LAS X, Leica Microsystems, Germany)

#### **Fig S4. The development of paclitaxel resistance is followed by the intracellular redistribution of Paclitaxel Oregon Green 488 and doxorubicin**

(A-B) Comparison of doxorubicin intracellular localization between non-resistant and paclitaxel-resistant cancer cell lines (A549 – A and MDA-MB-231 – B) after their exposure to doxorubicin (0.05  $\mu\text{M}$ ; 24 h; red). The lysosomes were stained with LysoTracker™ Deep Red (green). DNA was stained with DAPI. Cells were observed using TCS SP8 (Leica Microsystems, Germany) confocal microscope (C) The colocalization of Paclitaxel Oregon Green 488 (0.1  $\mu\text{M}$ ), endoplasmic reticulum and Golgi apparatus in non-resistant and paclitaxel-resistant A549 cells was monitored by staining of the latter organelles with BODIPY™ TR Ceramide (red) and pictures were acquired using TCS SP8 (Leica Microsystems, Germany) confocal microscope. DNA was counterstained with DAPI. (E) The colocalization of Paclitaxel Oregon Green 488 (0.1  $\mu\text{M}$ ), and mitochondria in non-resistant and paclitaxel-resistant A549 cells was monitored by staining of the mitochondria with MitoTracker™ Red FM (red) and pictures were acquired using TCS SP8 (Leica Microsystems, Germany) confocal microscope. DNA was counterstained with DAPI. Correlation of Paclitaxel Oregon Green 488 and

endoplasmic reticulum/ Golgi apparatus (D) and LysoTracker (F) occurrence was quantified with Leica Application Suite X. The difference between two means was tested with Student's t-test and statistically significant differences are marked with \* when  $p < 0.05$ , \*\* when  $p < 0.01$ , \*\*\* when  $p < 0.001$ .

**Fig S5. Lysosomotropic neutralizing agent prevents ABCC-dependent drug sequestration in lysosomes of paclitaxel-resistant cancer phenotypes**

A) The impact of lysosomotropic neutralizing agent (ammonium chloride - AC; 25 mM, 2 h prior to anthracyclin) and pan-ABCC inhibitor (MK-571; 25  $\mu$ M; 2 h prior to anthracyclin) on the intracellular codistribution of doxorubicin (red) and lysosomes (LysoTracker™ Deep Red - green) in cells cultured in monolayer was observed using TCS SP8 (Leica Microsystems, Germany) confocal microscope. DNA was stained with DAPI (blue). (B) The depth of penetration of 3 week old A549-PTX spheroid culture by doxorubicin (0.05  $\mu$ M; 24 h; red), co-stained with LysoTracker™ Deep Red (75 nM; 2 h; green) and DAPI (1  $\mu$ g/ml; 30 min; blue), with and without Ammonium chloride - AC (25 mM; 2 h prior to doxorubicin). The spheroids was analyzed with Leica Application Suite X on pictures captured with confocal microscope (TCS SP8, Leica Microsystems, Germany). Red fluorescence intensity (ex: 470 and em: 580-600 nm) that corresponds to drug concentration was monitored across spheroid section. (C,D) The depth of penetration of 3 week old A549-PTX spheroid culture by doxorubicin (C) (0.05  $\mu$ M; 24 h; red) and (D) Paclitaxel Oregon Green™ 488 (0,1  $\mu$ M), co-stained with DAPI (1  $\mu$ g/ml; 30 min; blue), with and without MK-571 - iABCC (25  $\mu$ M). The spheroids was analyzed with Leica Application Suite X on pictures captured with confocal microscope (TCS SP8, Leica Microsystems, Germany). Paclitaxel Oregon Green™ fluorescence that corresponds to drug concentration was monitored across spheroid section. (E) The role of ABCC in cell protection against doxorubicin-induced cytotoxicity (0.05  $\mu$ M; 48 h) in 3D culture of 3 week old A549-PTX spheroids was assayed by spheroid triple staining with Annexin V (green), propidium iodide (red) and DAPI (blue) for 1 h. iABCC was added as in (C,D). Images were acquired as in B, C and D. The green fluorescence intensity of entire spheroid corresponds to the extent of apoptosis in the culture, whereas intensity of red fluorescence to necrosis.

**Fig S6. The efficacy of ABCC3, ABCC5 and ABCC10 targeting with siRNA and lack of siRNA cross-reactivity**

(A) Whole cell lysates derived from 2D cell cultures transfected with siRNA against mRNA of ABCC3, ABCC5, ABCC10 and equal molar mixture of all for 72 h were separated using SDS-PAGE. Membranes were stained with anti-ABCC3, anti-ABCC5 and anti-ABCC10 antibodies to confirm selectivity and efficacy of particular siRNAs. Cells transfected with non-template siRNA (siCTRL) served as a control for normal protein level. ACTB was used as a loading control.

**Fig S7. The deficiency of ABCC3, ABCC5 and ABCC10 favors extra-lysosomal localization of doxorubicin**

(A) Intracellular localization of doxorubicin (0.05  $\mu$ M; 24 h; red) was monitored in cells proficient and deficient in particular ABCC transporters, which were treated with anthracyclin 72 h after transfection with corresponding siRNA. Lysosomes were stained with LysoTracker™ Deep Red (green) and DNA with DAPI.

**Fig S8. The silencing of ABCC3, ABCC5 and ABCC10 declines accumulation of Paclitaxel Oregon Green 488 in lysosomes**

(A) Accumulation of Paclitaxel Oregon Green 488 in lysosomes of paclitaxel-resistant A549 cells proficient and deficient in ABCC3, ABCC5 and ABCC10 was evaluated by measuring fluorescence intensity of isolated lysosomes by LSR® II (Becton Dickinson) flow cytometer at ex: 496 nm/em: 524 nm. First, cells were transfected with siRNA for 72 h and then exposed to the fluorescently-labeled paclitaxel (0.1  $\mu$ M) for another 24 h. Lysosomes were isolated and fluorescence was read immediately. Lysosomes of siCTRL untreated cells served as background control for lysosome autofluorescence. Numerical values for each cell phenotype in legend (blue and pink boxes)

represent median value of fluorescence distribution.

**Fig S9. Simultaneous deficiency of ABCC3, ABCC5 and ABCC10 sensitizes paclitaxel-resistant cells to doxorubicin**

(A and B) Intracellular distribution of doxorubicin (0.05  $\mu$ M; 24 h; red) was tested 72 h after paclitaxel-resistant transfection of A549 (A) and MDA-MB-231 (B) with the equal molar mixture of siABCC3, siABCC5 and siABCC10 or non-template control. Lysosomes were stained with LysoTracker<sup>TM</sup> Deep Red (green), whereas DNA with DAPI (blue). (C) Colocalization of green and red fluorescence was analyzed and quantified in Leica Application Suite X. (D) 4 week-old 3D PTX-resistant A549 were transfected with mix of ABCC3, ABCC5 and ABCC10 or siRNA control 72 h prior to treatment with doxorubicin (0,05  $\mu$ M; 24 h; red), stained with LysoTracker<sup>TM</sup> Deep Red (green) and DAPI (blue). Spheroid fluorescence was captured with confocal microscope (TCS SP8, Leica Microsystems, Germany). The fluorescence intensity plot at spheroid cross section was determined in arbitrary units (a.u.) with Leica Application Suite X.

**Fig S10. ABCC3, ABCC5 and ABCC10 silencing increase proapoptotic effect of doxorubicin and paclitaxel in 3D cancer cell models**

(A,B) The role of ABCC3, ABCC5 and ABCC10 in cell protection against paclitaxel-induced cytotoxicity (0.1  $\mu$ M; 48 h) in 3D culture of 4 week old A549-PTX (A) and MDA-MB-231 (B) spheroids was assayed by spheroid triple staining with Annexin V (green), propidium iodide (red) and DAPI (blue) for 1 h. The spheroids was transfected with siRNA against mRNA of ABCC3, ABCC5, ABCC10 and equal molar mixture of all for 72 h. (C,D) The role of ABCC3, ABCC5 and ABCC10 in cell protection against doxorubicin -induced cytotoxicity (0.05  $\mu$ M; 48 h) in 3D culture of 4 week old A549-PTX (C) and MDA-MB-231 (D) spheroids was assayed by spheroid triple staining with Annexin V (green), propidium iodide (red) and DAPI (blue) for 1 h. The spheroids was transfected with siRNA against mRNA of ABCC3, ABCC5, ABCC10 and equal molar mixture of all for 72 h.

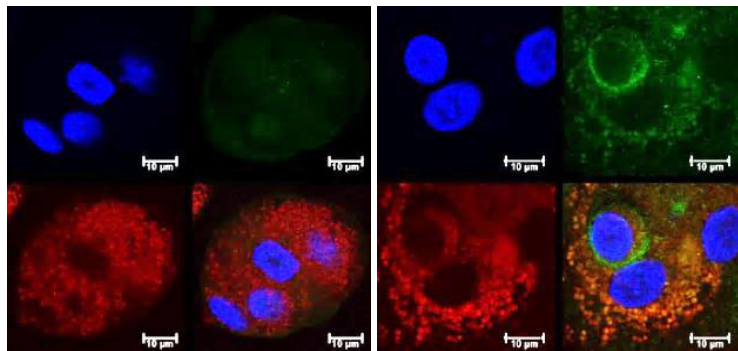
Fig. S1

A

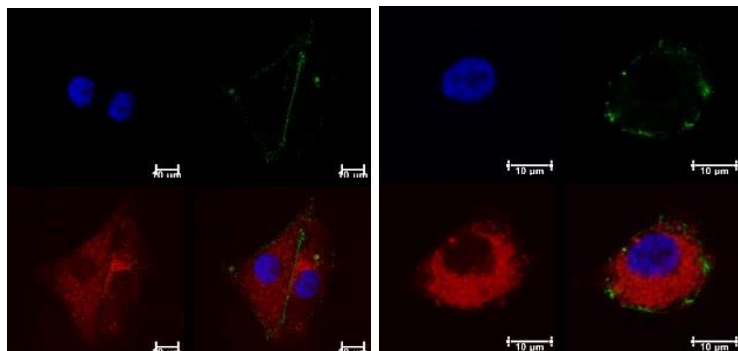
A549

A549-PTX

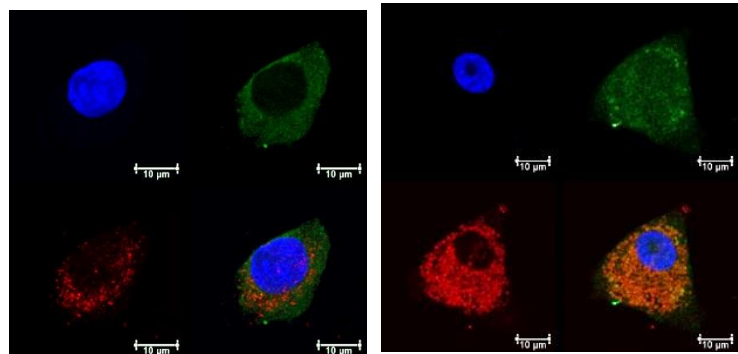
ABCB1



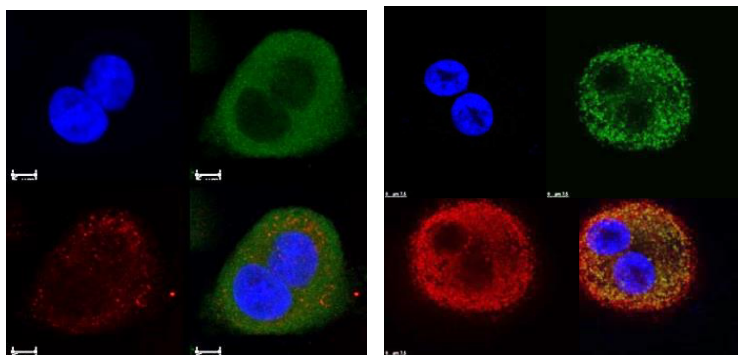
ABCC1



ABCC3



ABCC10



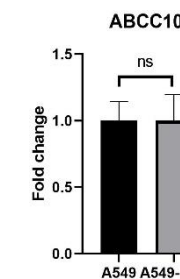
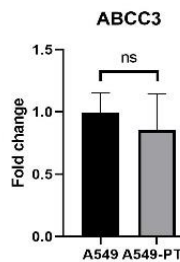
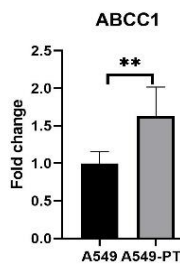
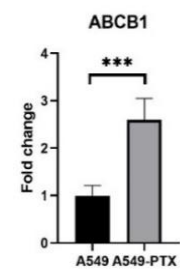
Nucleus

ABC transporters

Lysosomes

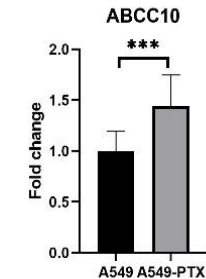
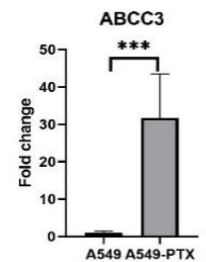
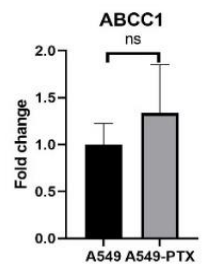
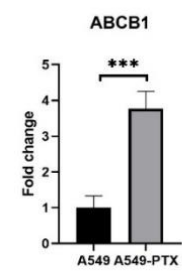
B

Protein expression level



C

Colocalization rate



D

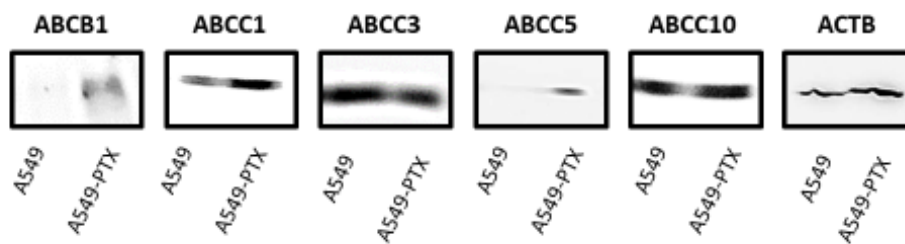
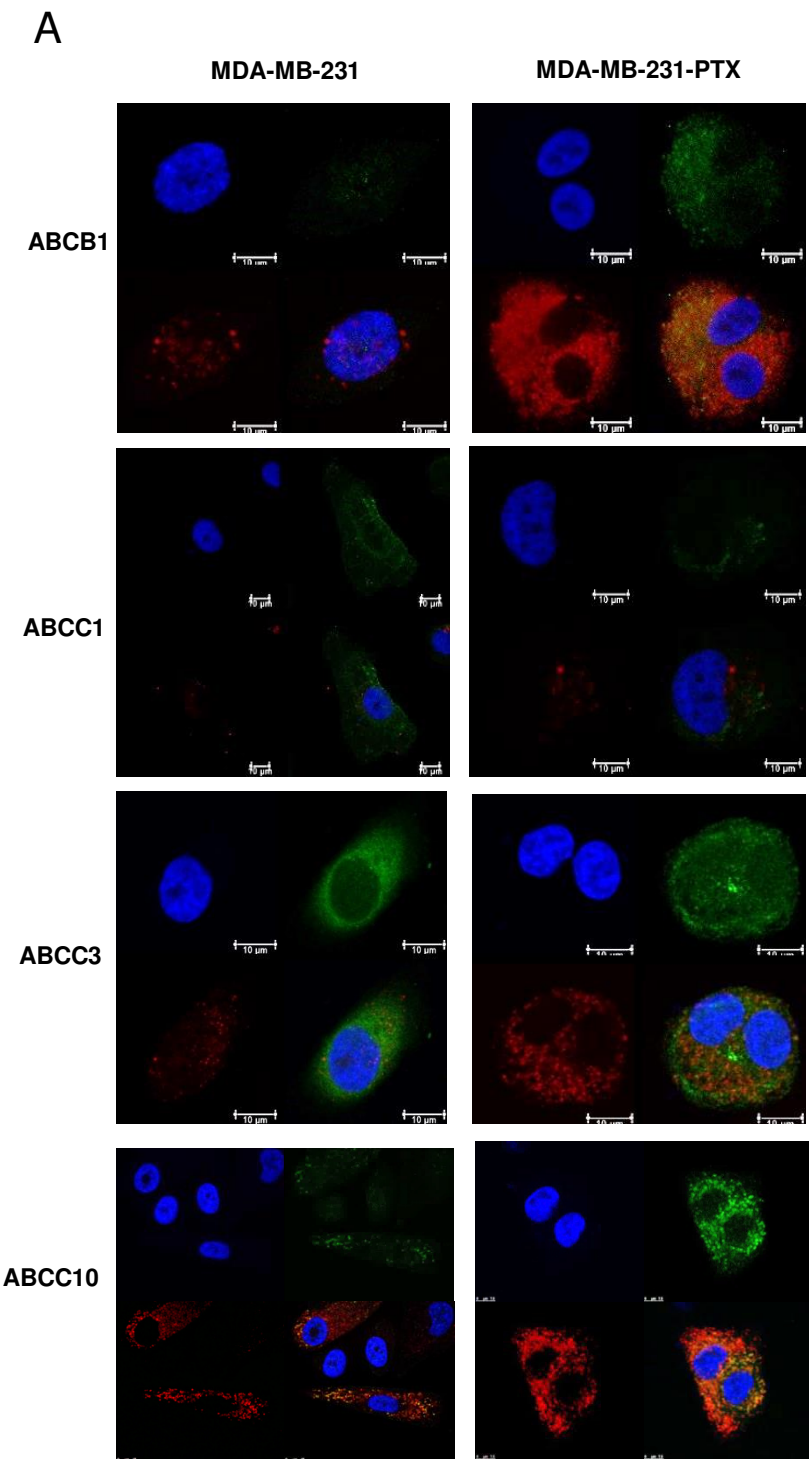
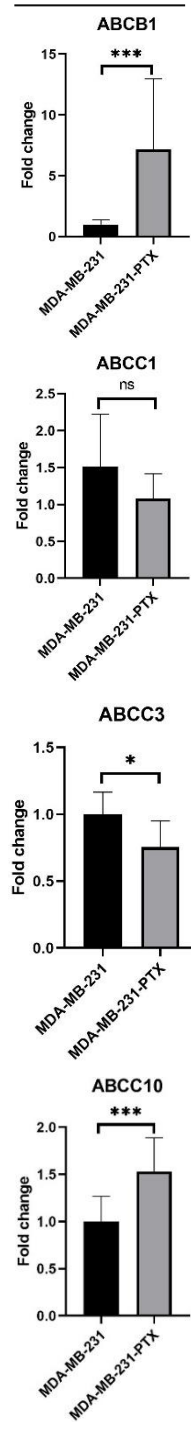


Fig. S2



**B Protein expression level**



**C Colocalization rate**

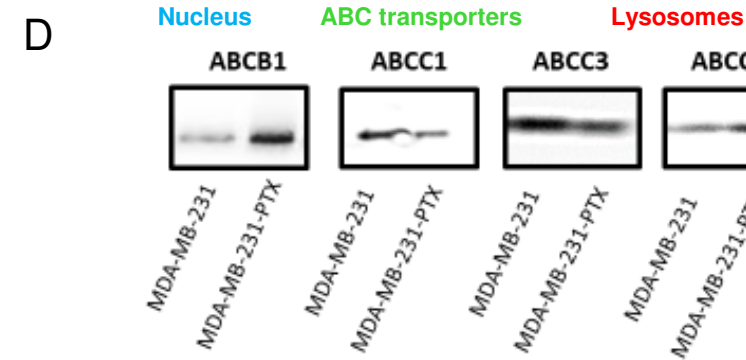
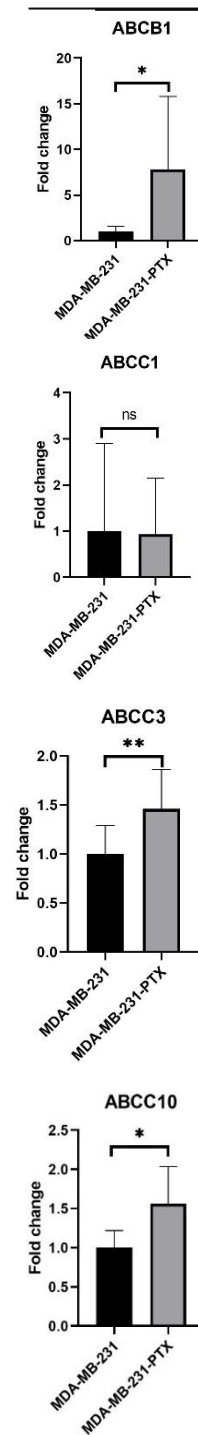


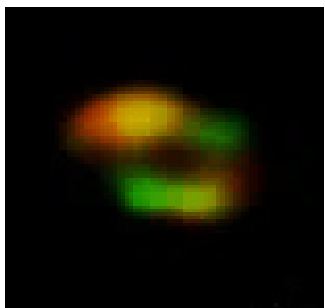
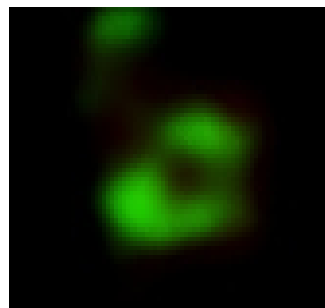
Fig. S3

A

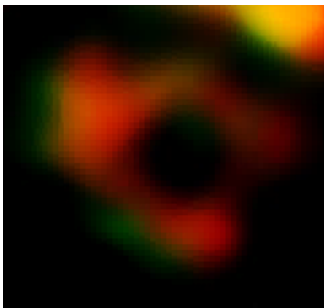
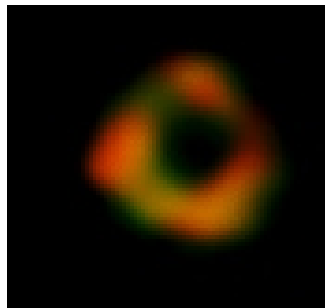
ABCC3

ABCC10

A549



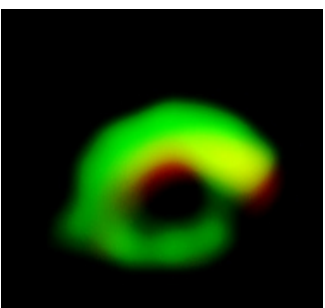
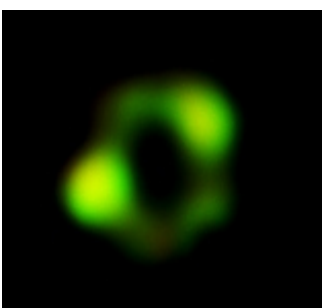
A549-PTX



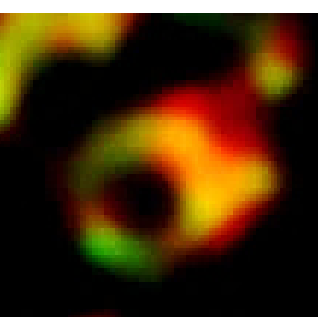
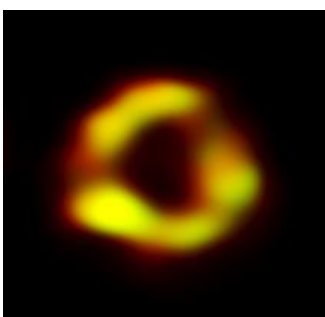
LAMP ABC transporters

B

MDA-MB-231



MDA-MB-231-PTX



LAMP ABC transporters

Fig. S4

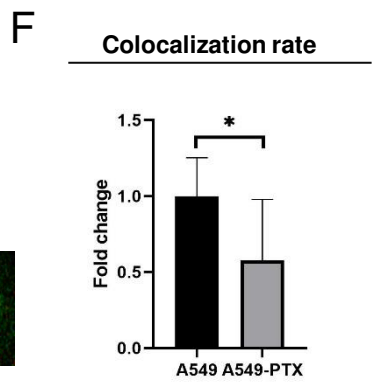
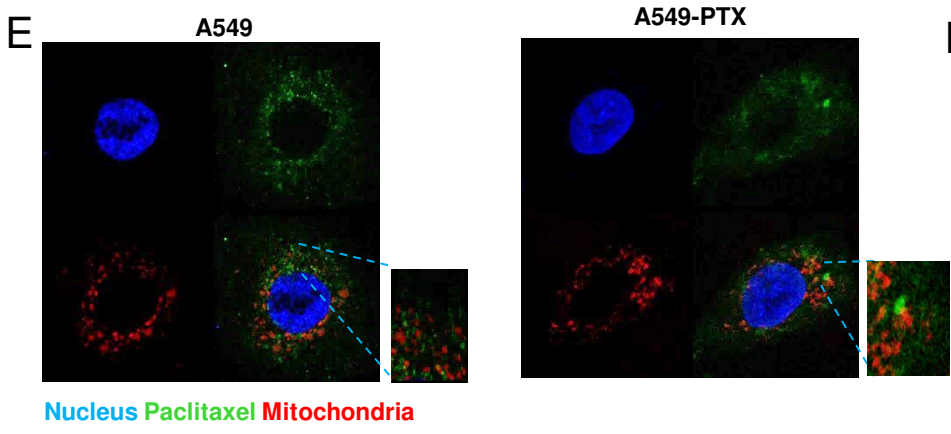
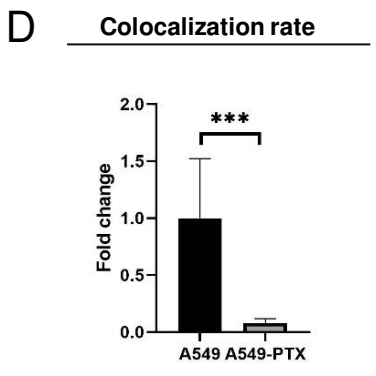
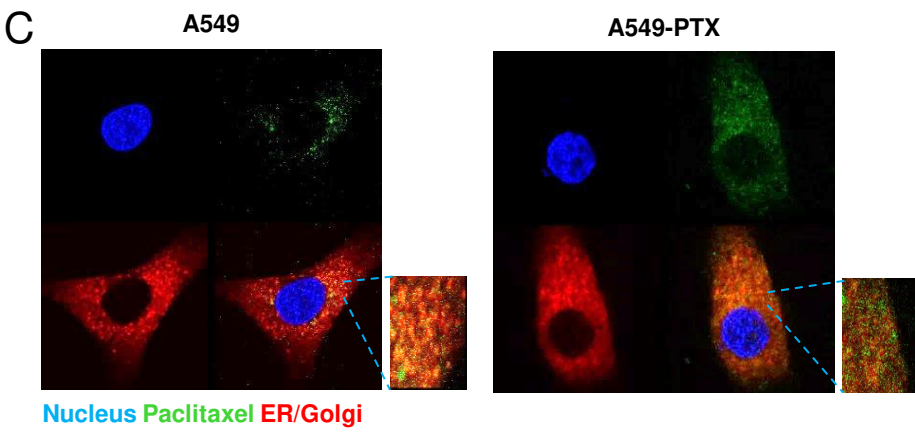
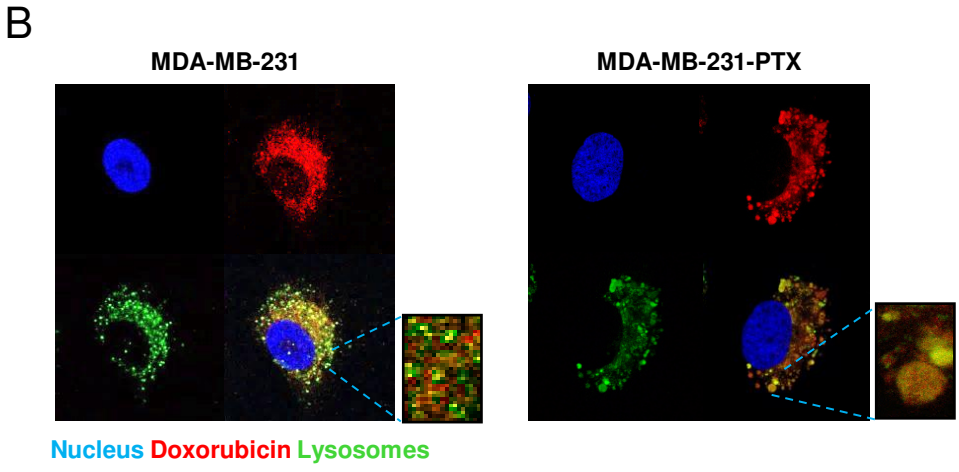
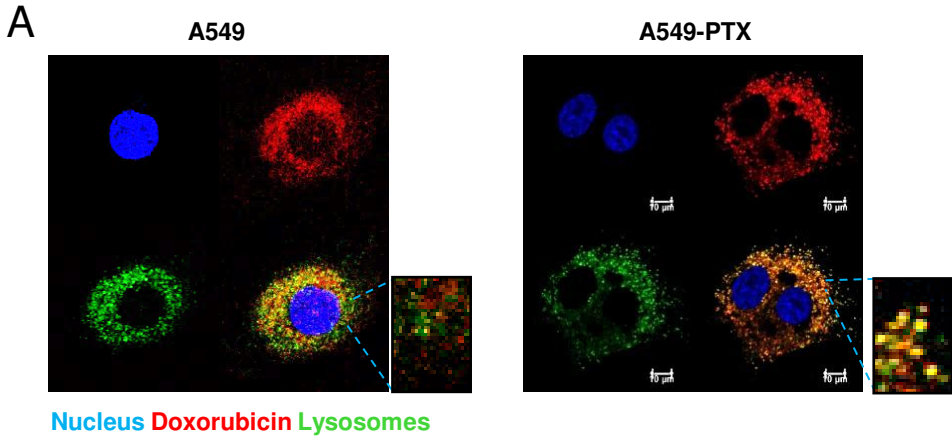
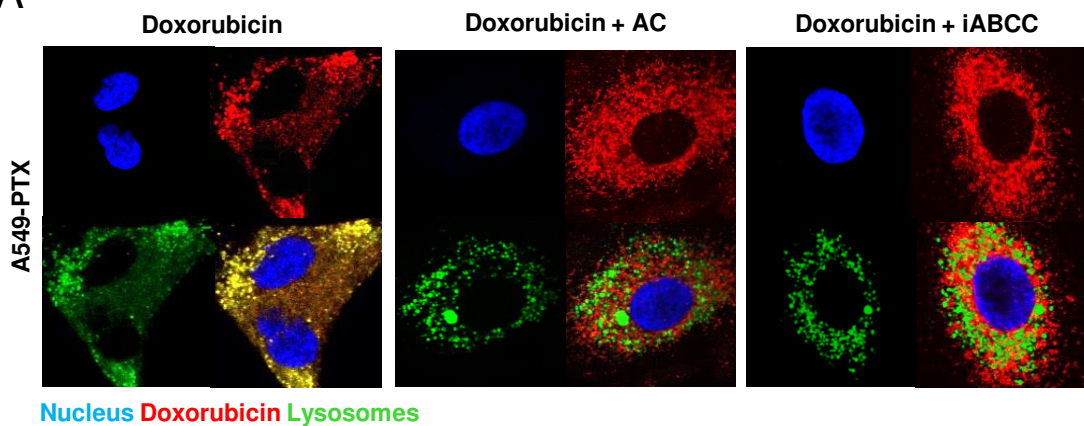
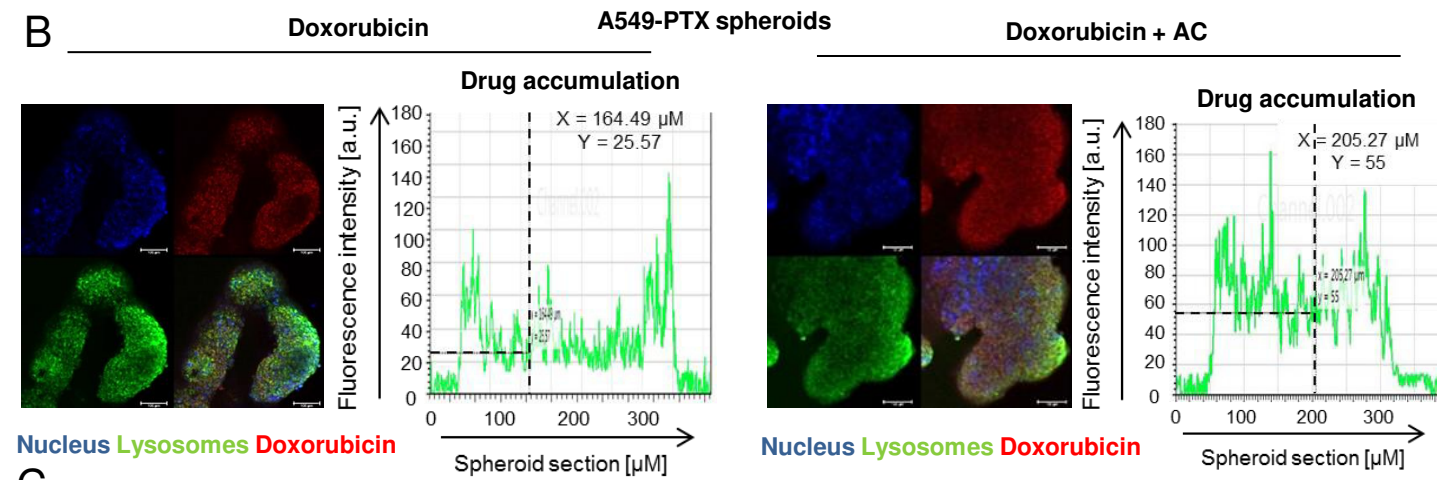


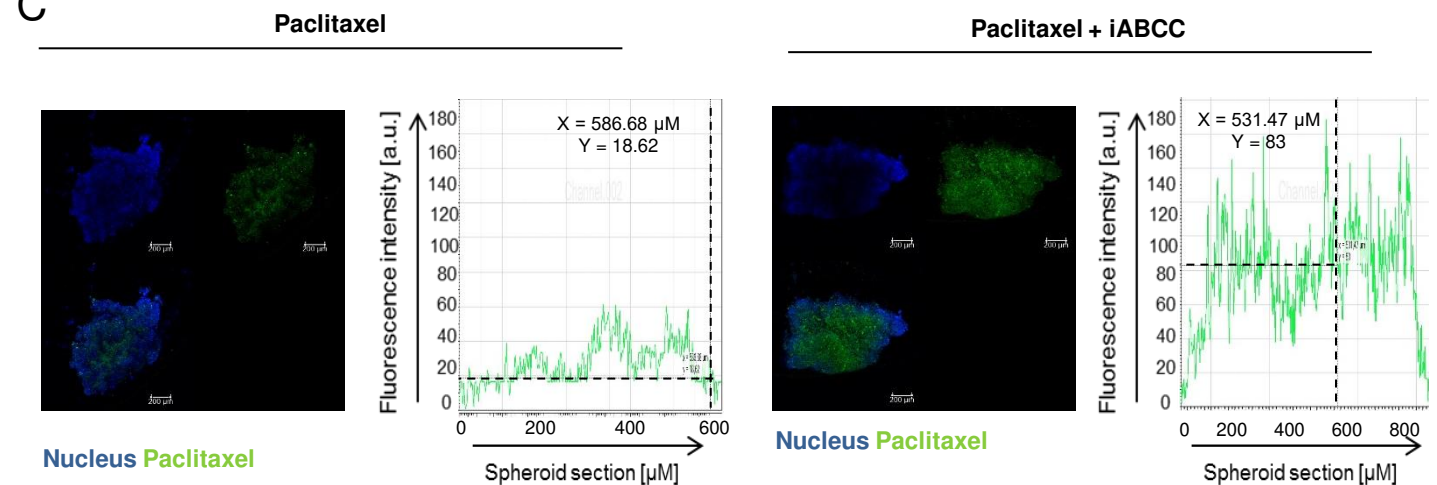
Fig. S5 A



**B**



**C**



**D**

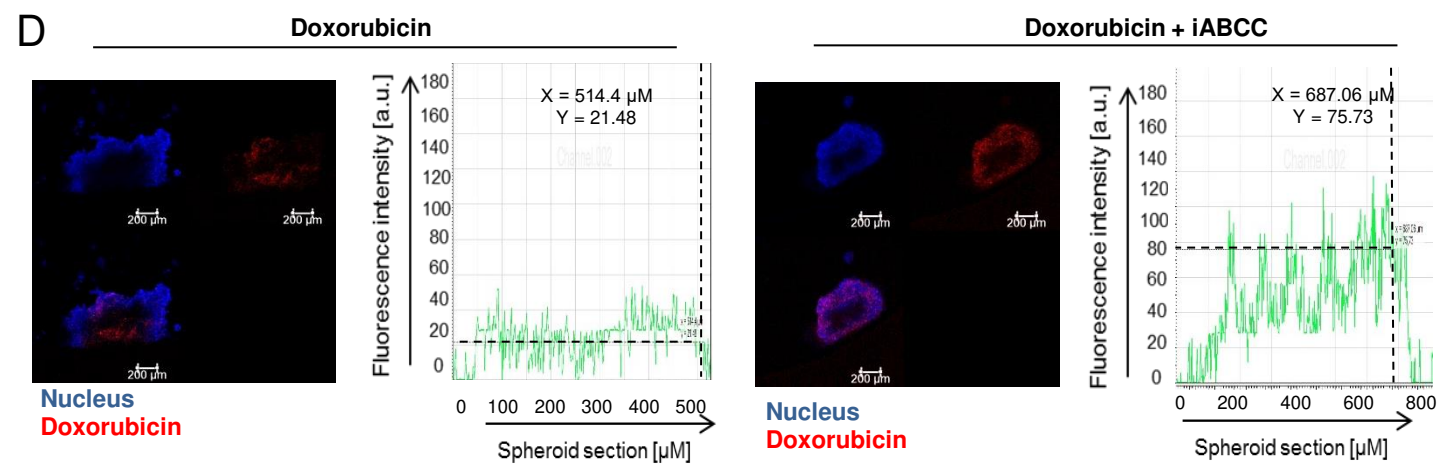


Fig. S5

E

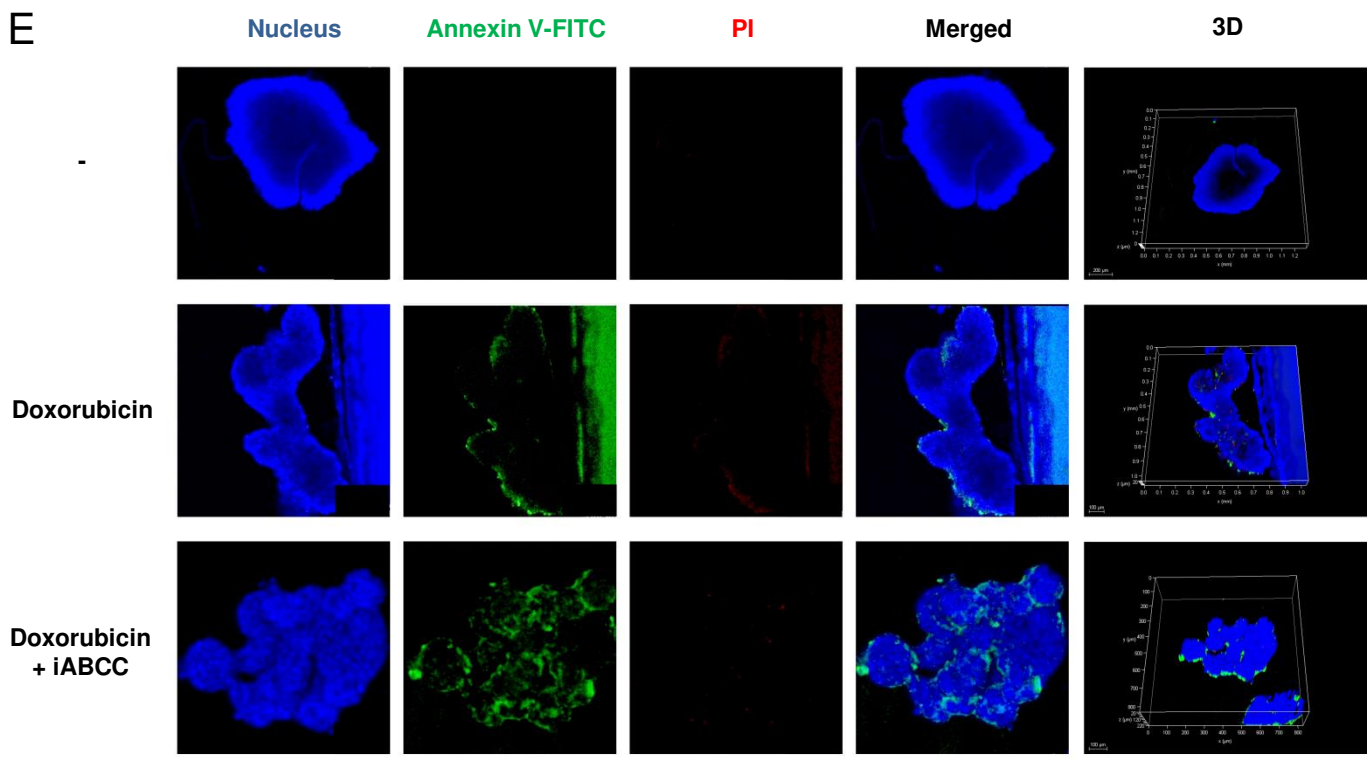


Fig. S6

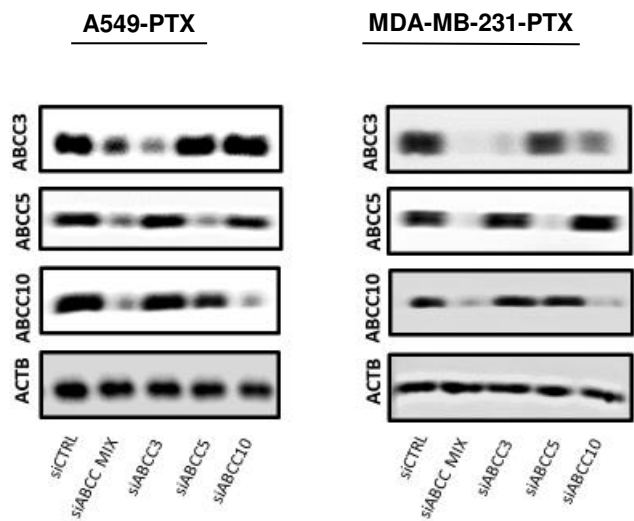


Fig. S7

MDA-MB-231-PTX + Paclitaxel

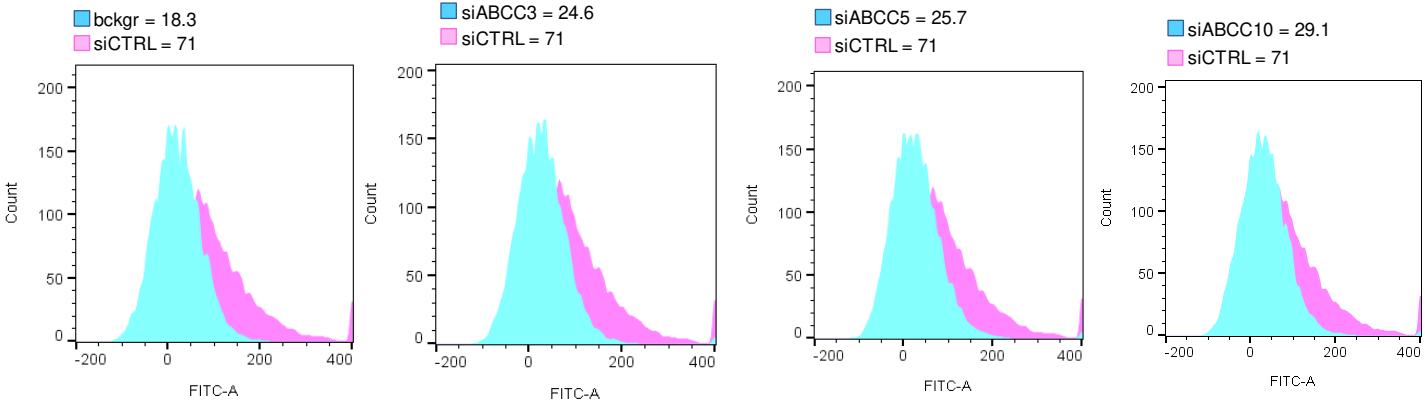


Fig. S8

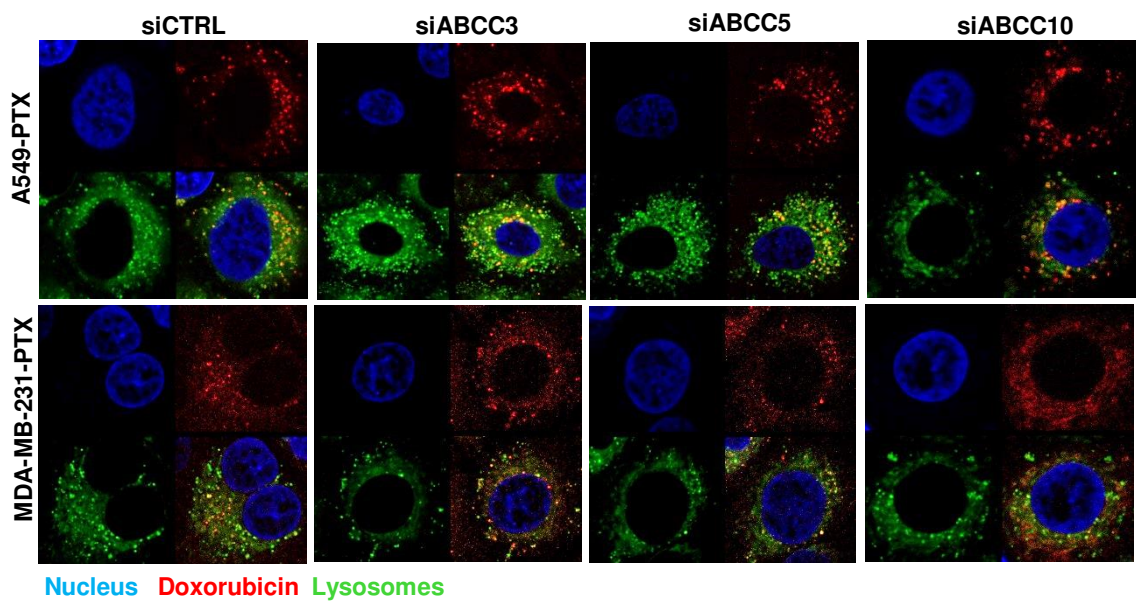


Fig. S9

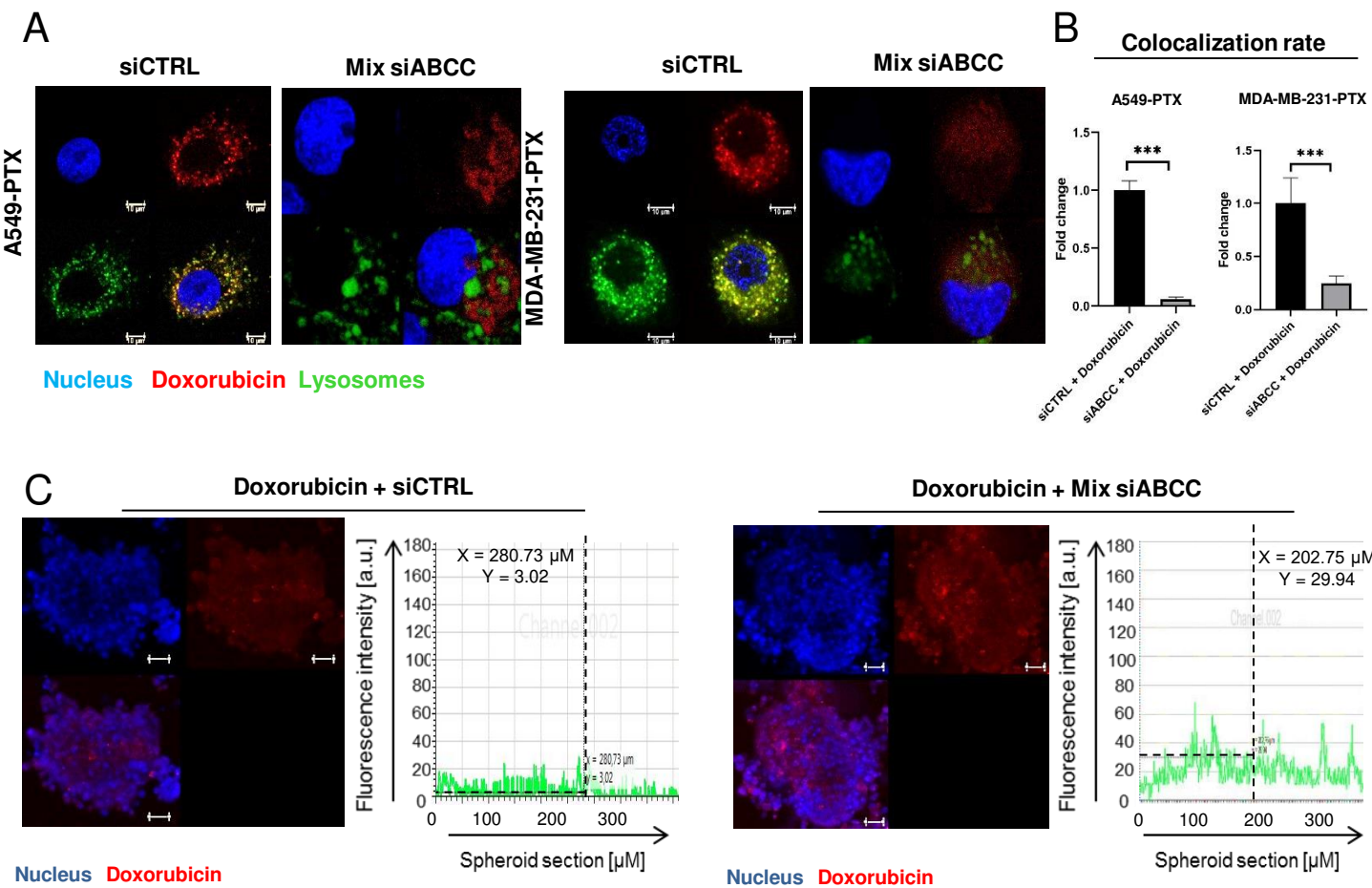
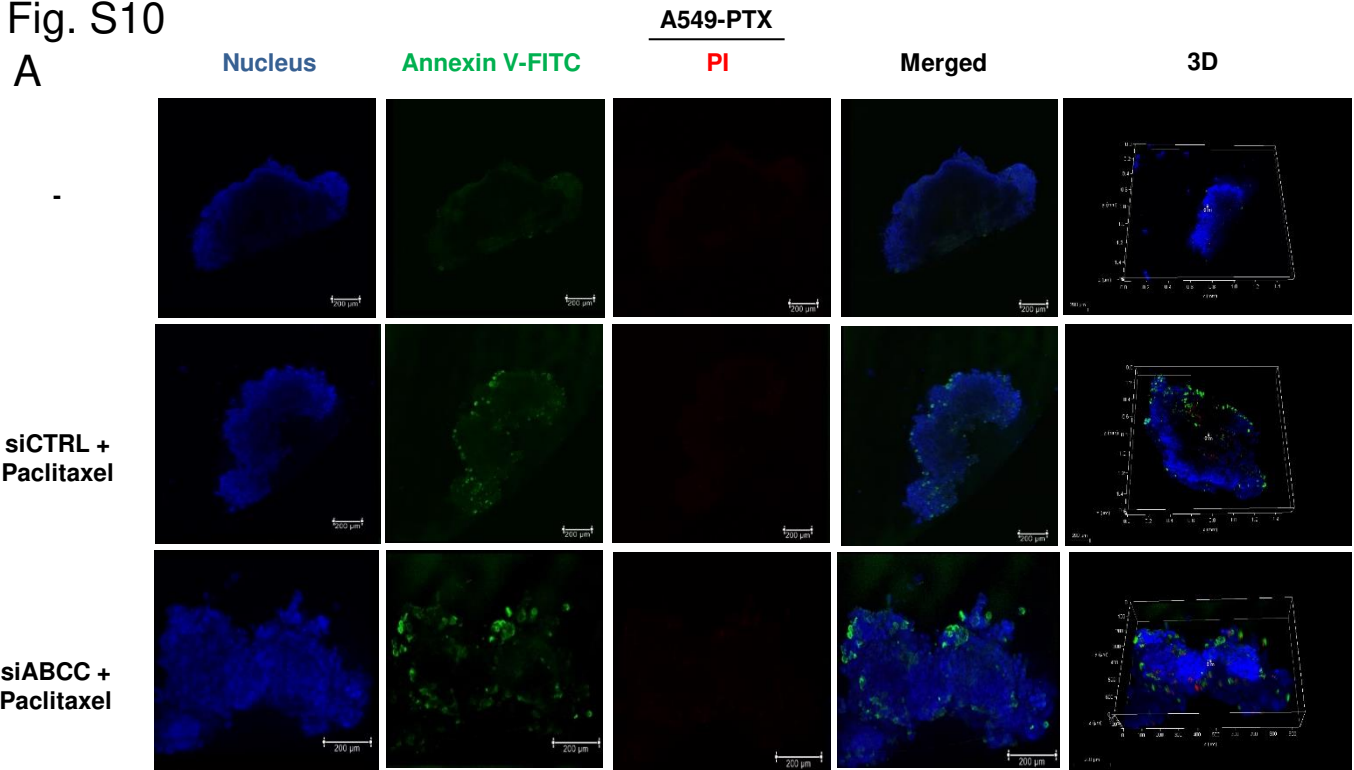


Fig. S10

A



B

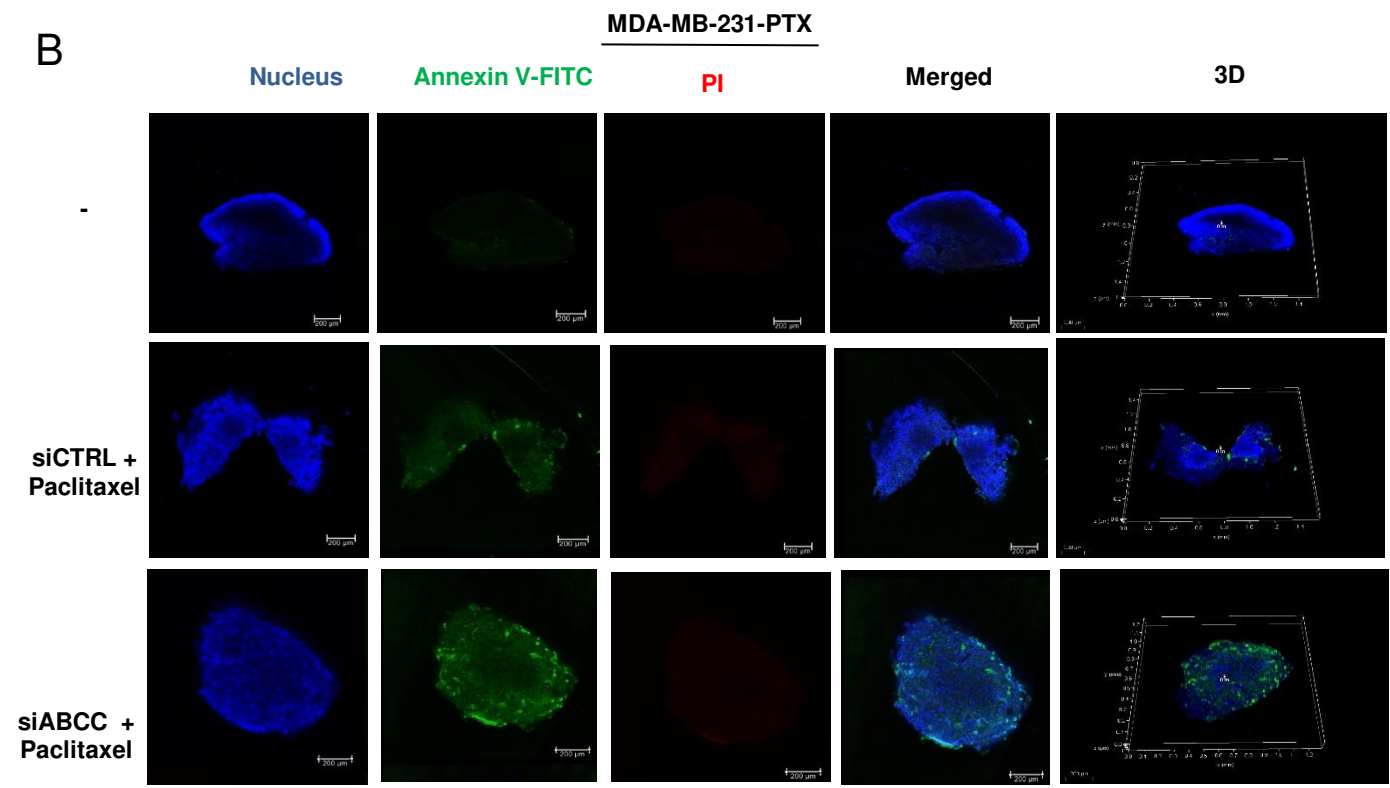


Fig. S10

A549-PTX

C

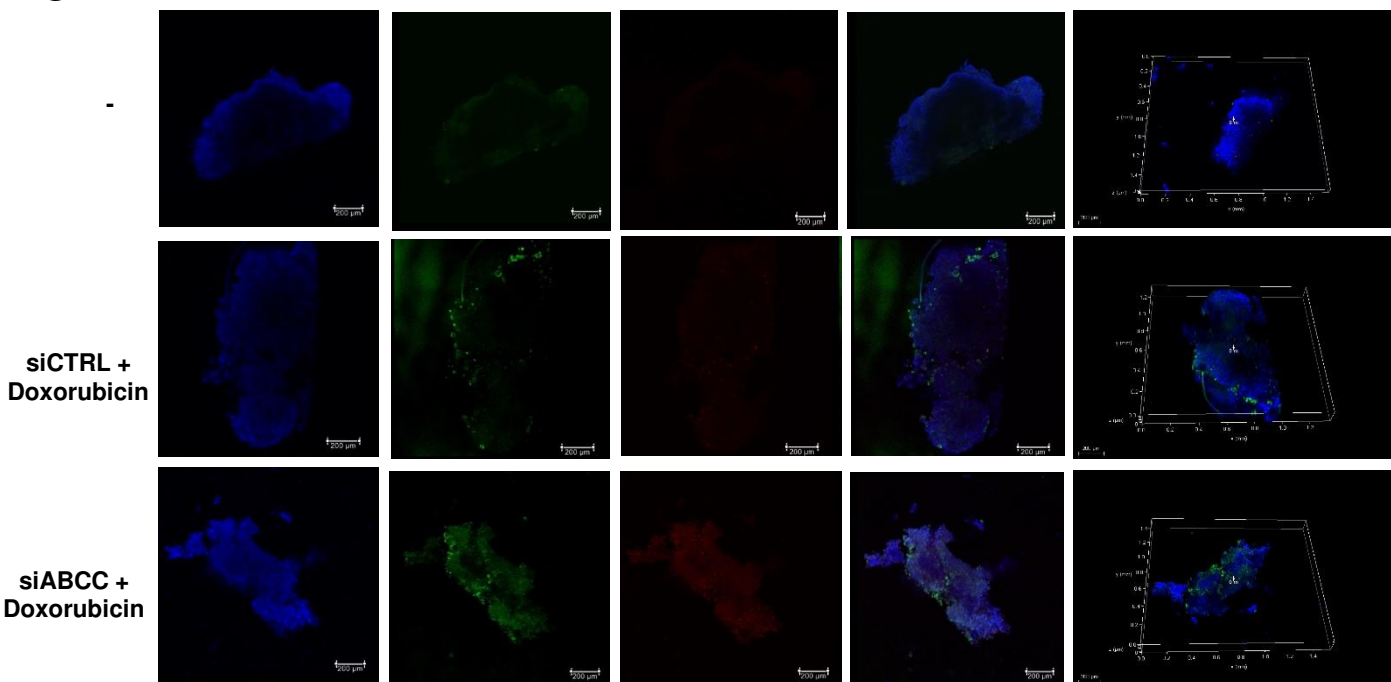
Nucleus

Annexin V-FITC

PI

Merged

3D



MDA-MB-231-PTX

D

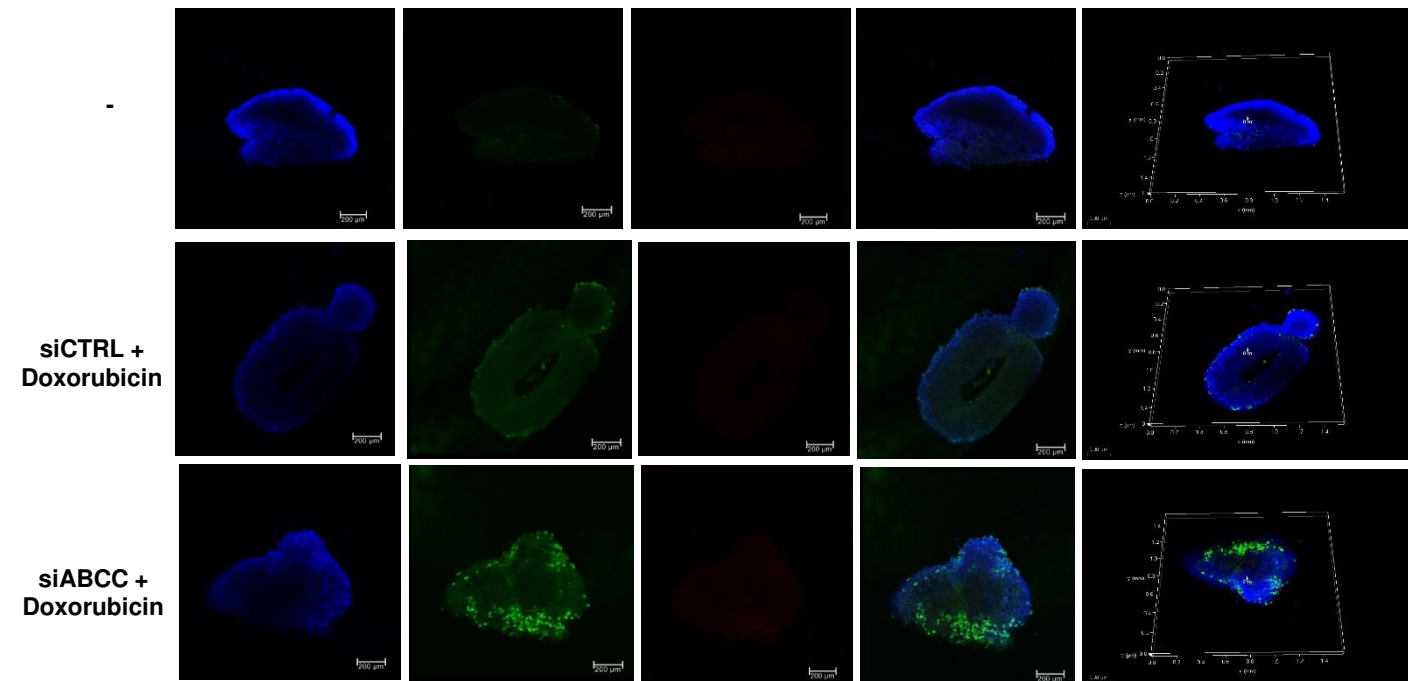
Nucleus

Annexin V-FITC

PI

Merged

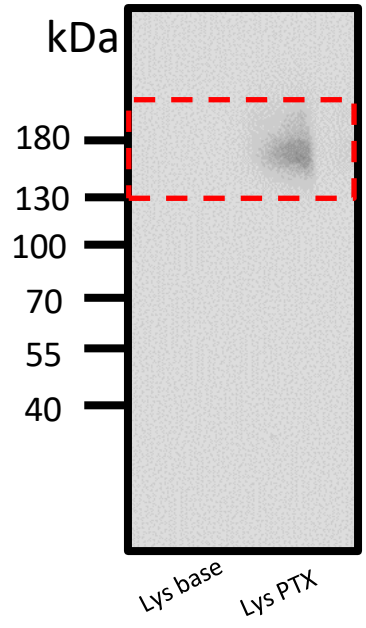
3D



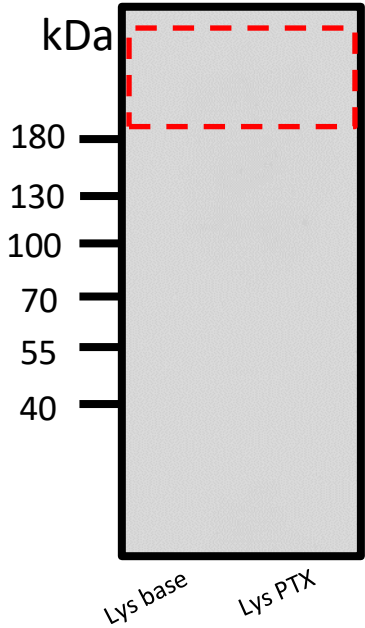
Lysosomes A549 vs A549-PTX

1D

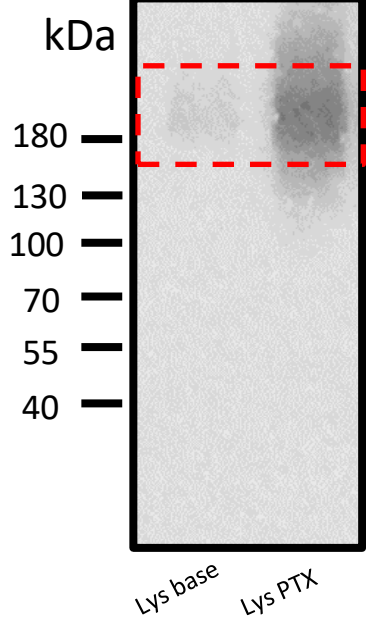
**ABCB1**



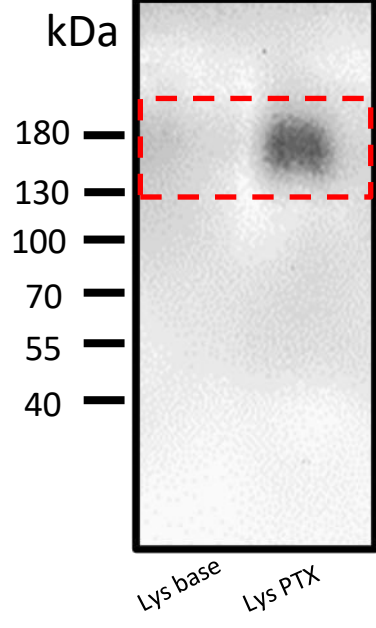
**ABCC1**



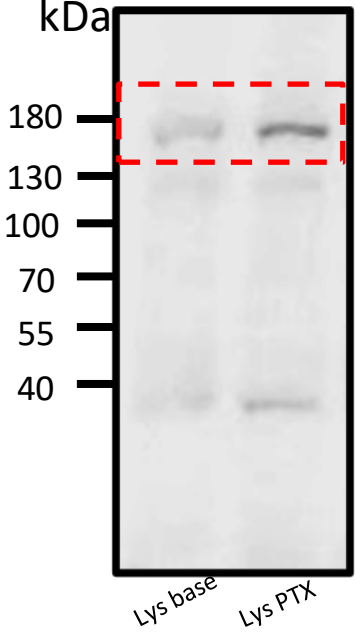
**ABCC3**



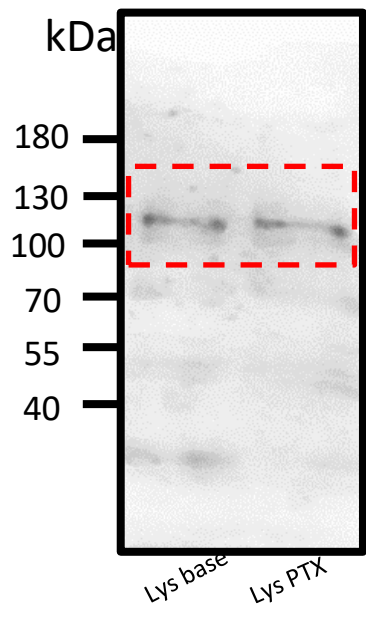
**ABCC5**



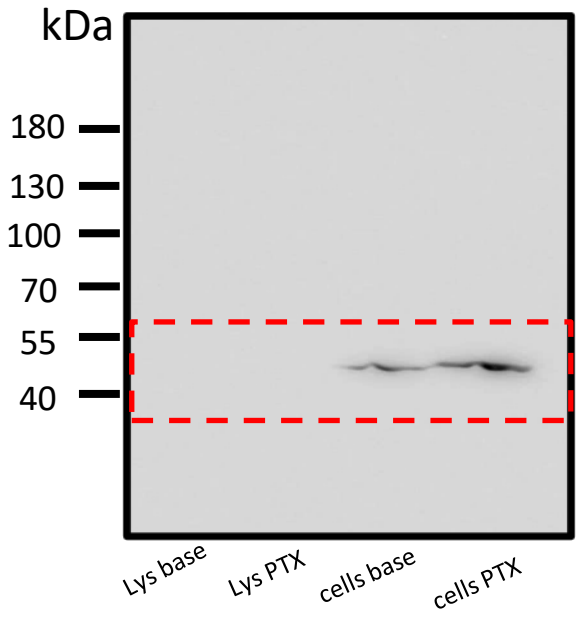
**ABCC10**



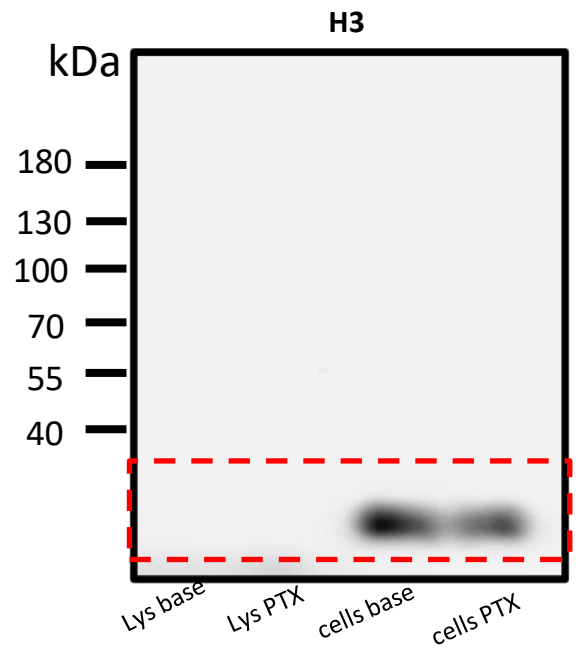
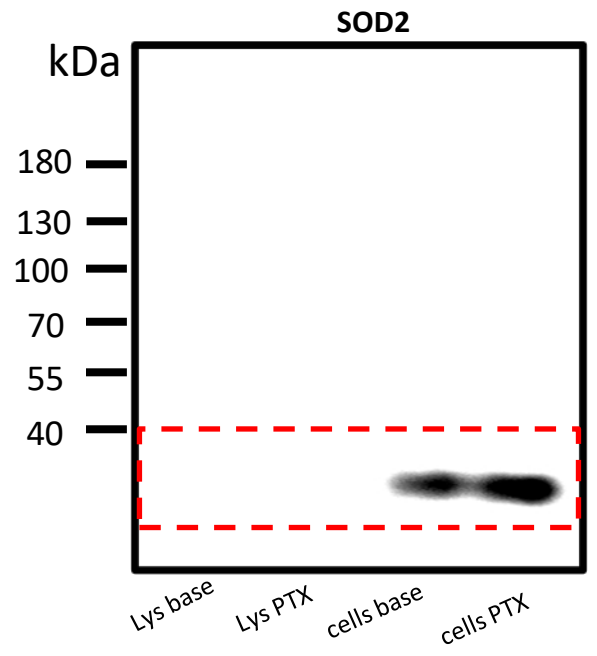
**LAMP**



**ACTB**

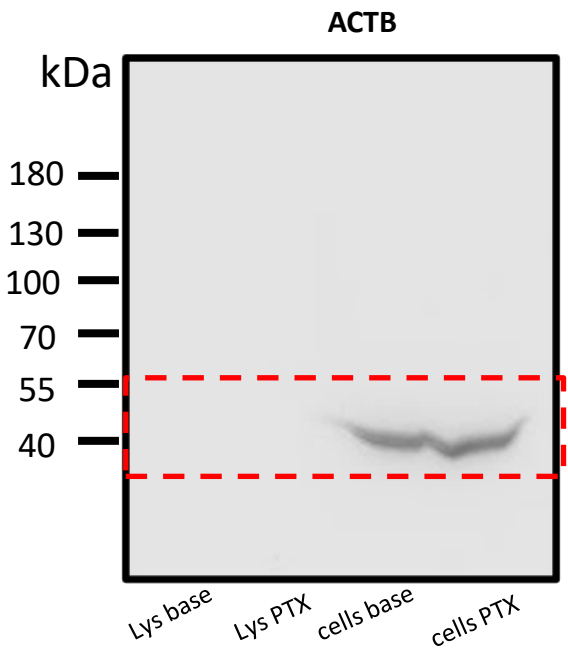
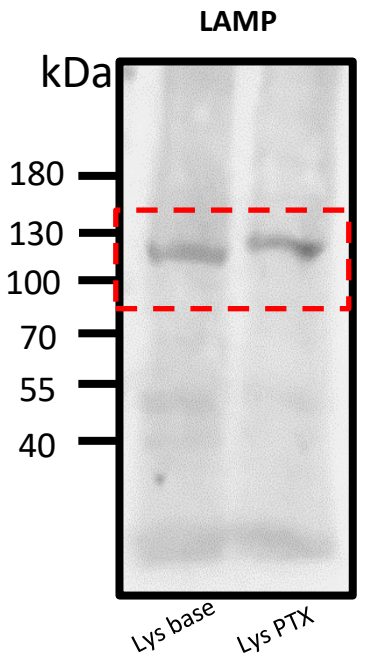
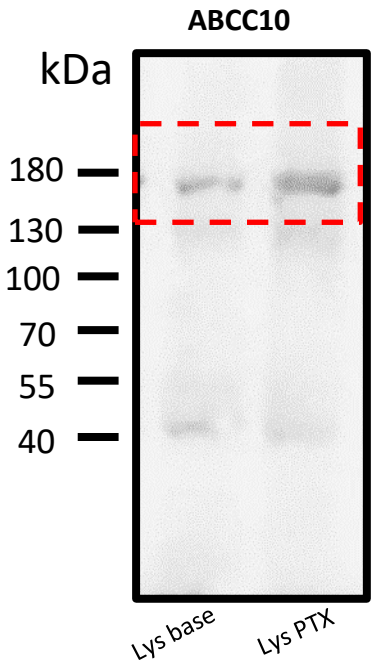
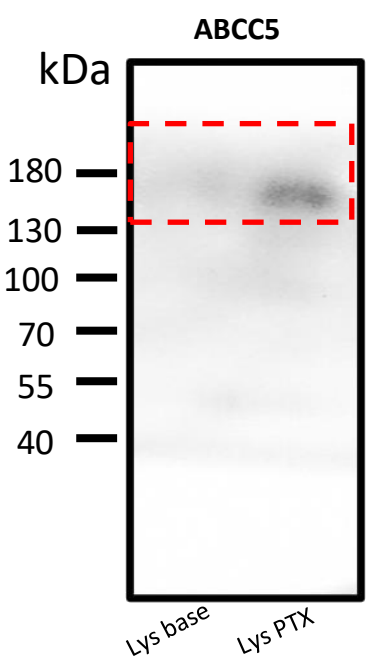
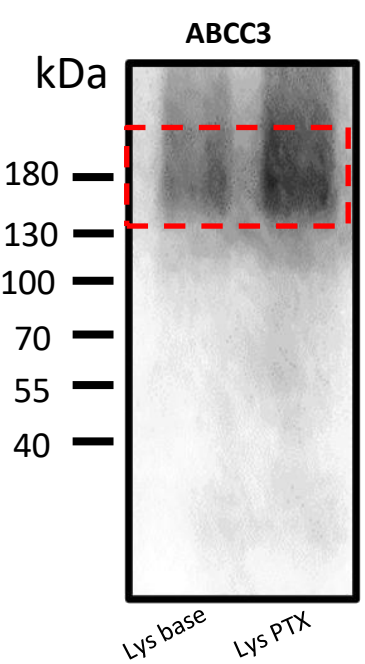
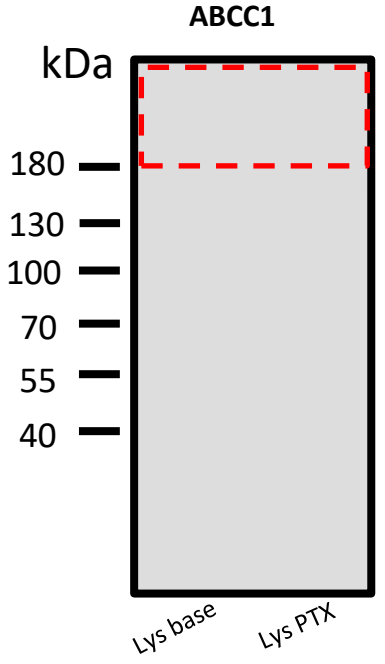
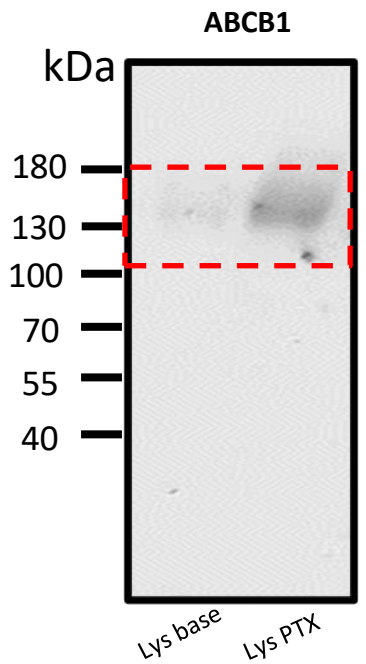


Lysosomes A549 vs A549-PTX

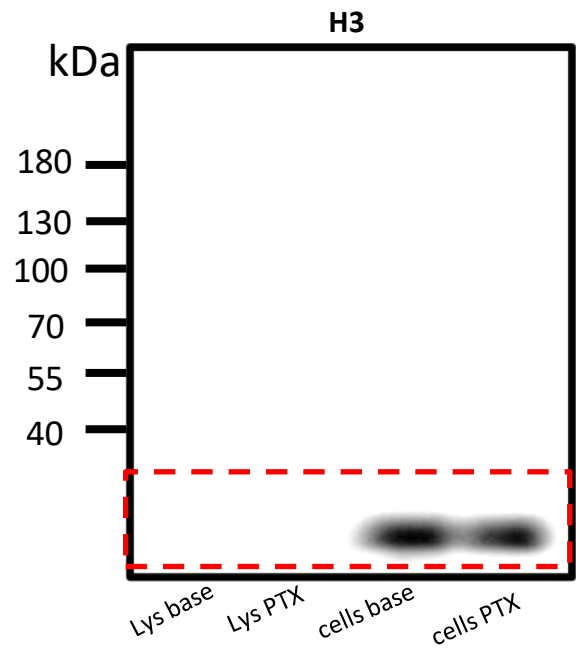
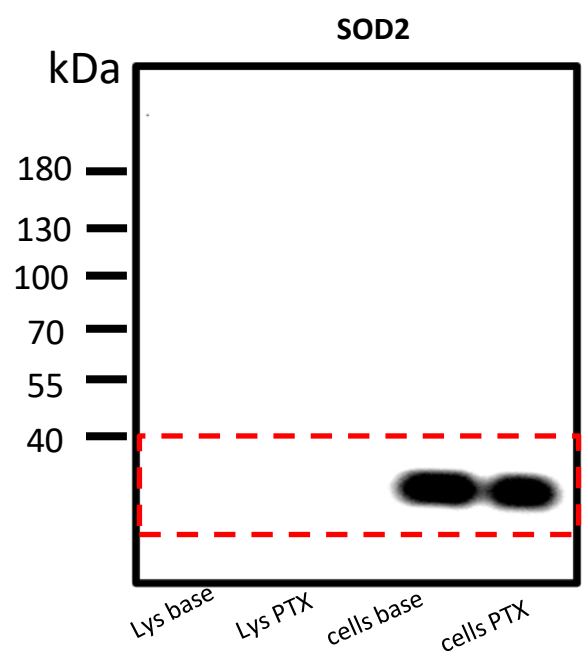


1H

Lysosomes MDA-MB-231 vs MDA-MB-231-PTX

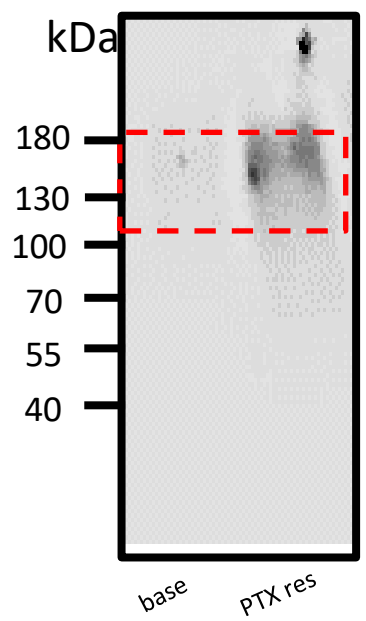


Lysosomes MDA-MB-231 vs MDA-MB-231-PTX

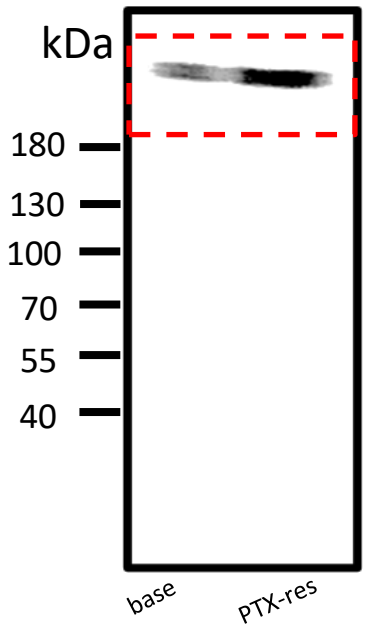


S1D Whole cel lysates A549 vs A549-PTX

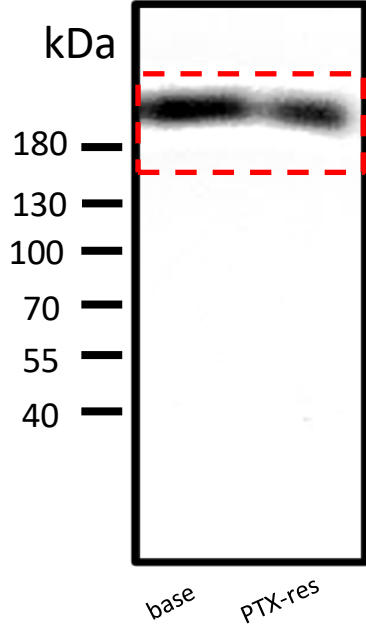
**ABCB1**



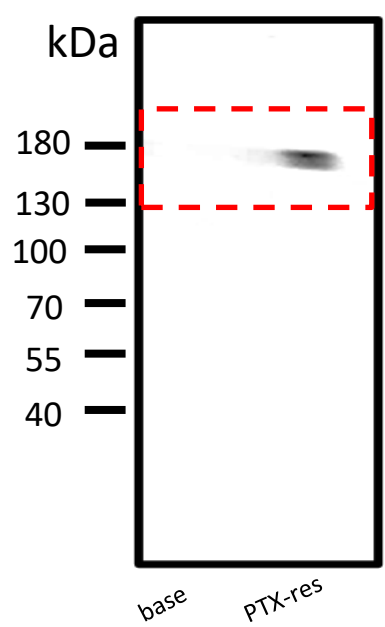
**ABCC1**



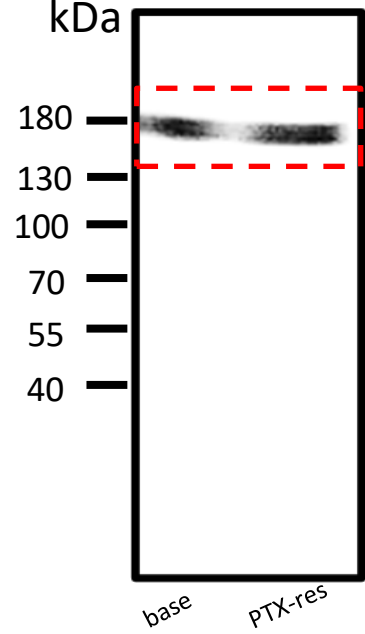
**ABCC3**



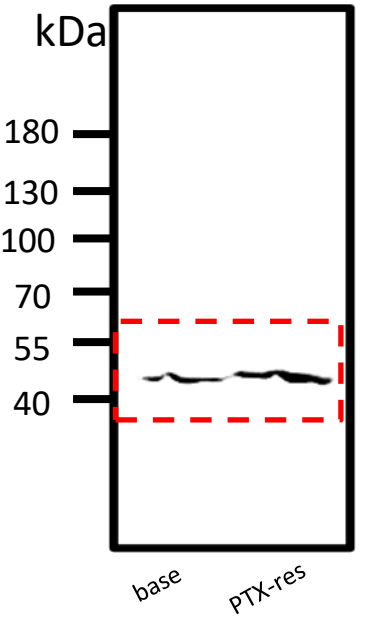
**ABCC5**



**ABCC10**



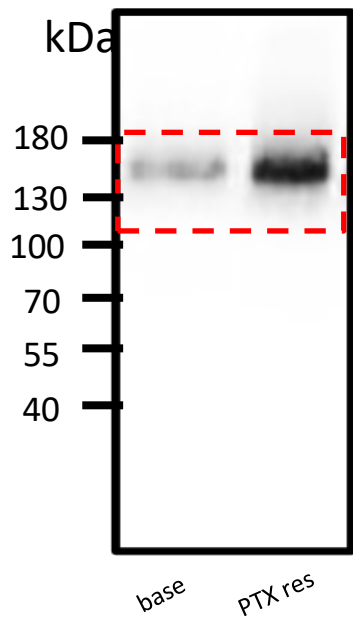
**ACTB**



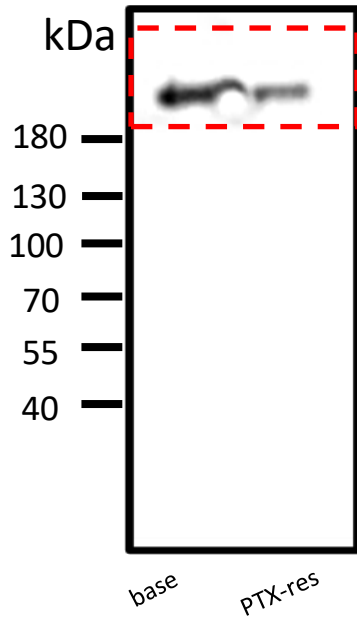
Whole cell lysates MDA-MB-231 vs MDA-MB-231-PTX

S2D

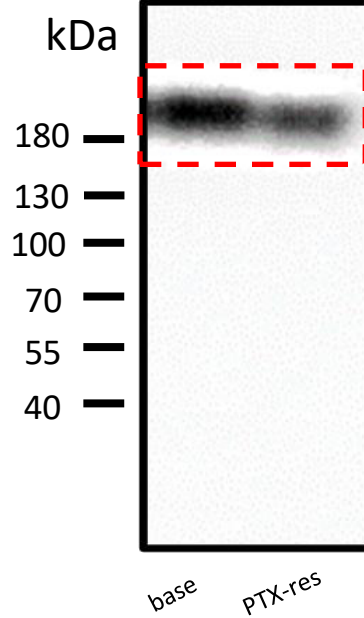
**ABCB1**



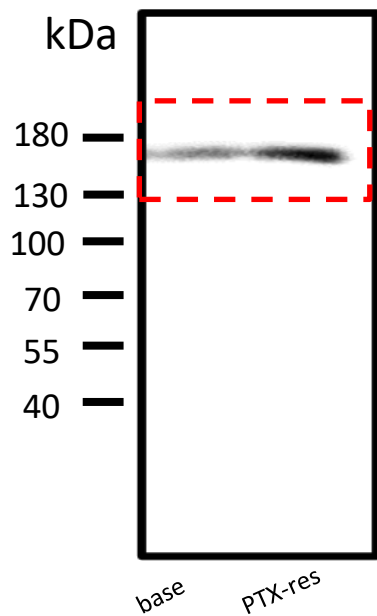
**ABCC1**



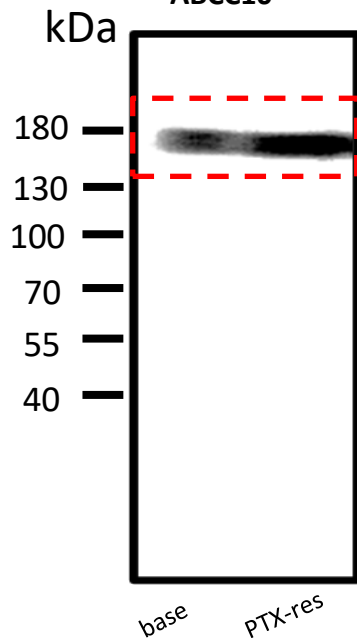
**ABCC3**



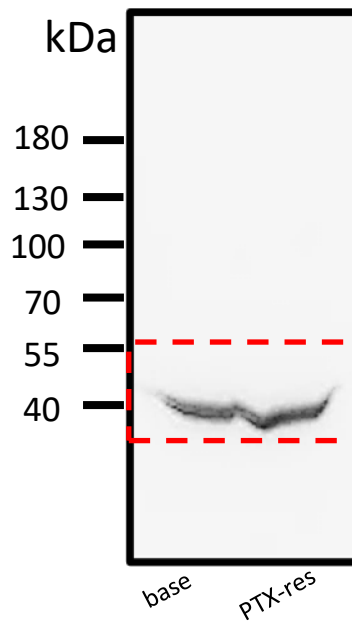
**ABCC5**



**ABCC10**



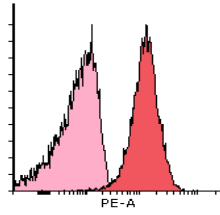
**ACTB**



# 2E-F

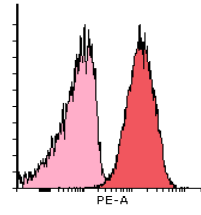
## A549

Median	
bckgr	57.04
Neutral Red	12 859.78



## A549-PTX

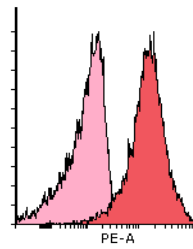
Median	
bckgr	76.90
Neutral Red	14 793.60



# 4E-F

## A549-PTX

Median	
bckgr	78.26
Neutral Red	15 098.72



## MDA-MB-231-PTX

Median	
bckgr	70.07
Neutral Red	14 510.86

